

# RSC Advances



This is an *Accepted Manuscript*, which has been through the Royal Society of Chemistry peer review process and has been accepted for publication.

*Accepted Manuscripts* are published online shortly after acceptance, before technical editing, formatting and proof reading. Using this free service, authors can make their results available to the community, in citable form, before we publish the edited article. This *Accepted Manuscript* will be replaced by the edited, formatted and paginated article as soon as this is available.

You can find more information about *Accepted Manuscripts* in the [Information for Authors](#).

Please note that technical editing may introduce minor changes to the text and/or graphics, which may alter content. The journal's standard [Terms & Conditions](#) and the [Ethical guidelines](#) still apply. In no event shall the Royal Society of Chemistry be held responsible for any errors or omissions in this *Accepted Manuscript* or any consequences arising from the use of any information it contains.

**Utilizing low ZIF-8 loading for asymmetric PSf/ZIF-8 mixed matrix  
membrane for CO<sub>2</sub>/CH<sub>4</sub> Separation**

*Nik Abdul Hadi Md. Nordin<sup>a</sup>, Ahmad Fauzi Ismail<sup>a,\*</sup>, Azeman Mustafa<sup>a</sup>, R. Surya Murali<sup>a</sup>,*

*Takeshi Matsuura<sup>b</sup>*

<sup>a</sup> Advanced Membrane Technology Research Centre (AMTEC), Universiti Teknologi Malaysia,  
81310 Skudai, Johor, Malaysia

<sup>b</sup> Industrial Membrane Research Laboratory, Department of Chemical and Biological  
Engineering, University of Ottawa, Ottawa, Ontario, Canada

\* Correspondence concerning this article should be addressed to Ahmad Fauzi Ismail (A. F. Ismail) at [afauzi@utm.my](mailto:afauzi@utm.my); [fauzi.ismail@gmail.com](mailto:fauzi.ismail@gmail.com)

## Abstract

Asymmetric mixed-matrix membranes (MMMs) were synthesized by incorporating zeolitic imidazole framework 8 (ZIF-8) into polysulfone (PSf) polymer matrix for CO<sub>2</sub>/CH<sub>4</sub> separation. ZIF-8 was synthesized in an aqueous media at room temperature with a base-type additive, triethylamine (TEA). The prepared ZIF-8 shows high crystallinity with a surface area of 1032 m<sup>2</sup>/g and particle size of ~133nm. MMMs were then prepared by incorporating the synthesized ZIF-8 up to 10wt% (total solids) into PSf via the dry/wet phase inversion. The prepared MMMs exhibit significant improvement in the thermal and mechanical stability even at the filler loading as low as 0.25wt%. Uniform dispersion of ZIF-8 throughout the PSf matrix was evident via SEM, up to 1 wt% filler loading. The permeation behavior of MMMs varies with the ZIF-8 loading; i.e. insignificant change was observed at the low filler loading (0.25wt%), while severe performance deterioration occurred at high filler loading (10wt%). At an optimal ZIF-8 loading of 0.5 wt%, CO<sub>2</sub> permeance was enhanced by 37% and CO<sub>2</sub>/CH<sub>4</sub> selectivity was also enhanced by 19% as compared to that of neat PSf membrane.

**Keywords:** Asymmetric mixed-matrix membrane, ZIF-8, PSf, low filler loading, CO<sub>2</sub>/CH<sub>4</sub> separation.

## 1 Introduction

Polymer membranes rise as a promising fluid separations media owing to their simplicity, modularity, low energy requirement and cost-effectiveness compared to conventional separations media<sup>1</sup>. Advent of asymmetric polymeric membranes, demonstrated by Loeb and Sourirajan, was the major breakthrough in the development of membrane processes<sup>2</sup>. Asymmetric membrane consists of a dense selective thin skin layer with a porous substructure as support, providing high permeation rate and high mechanical strength compared to the conventional dense membrane. The implementations of asymmetric membranes are highly demonstrated various separation aspects. In the last few decades, membrane technology for gas separation has been widely applicable for various applications such as acid gas purification, CO<sub>2</sub> separation from power plant flue gas, O<sub>2</sub> and N<sub>2</sub> enrichment and olefin/paraffin separation<sup>3</sup>.

Although polymeric membranes for gas separation are considered as preferable separation technique, they are constricted by the trade-off limits between permeability and selectivity<sup>4</sup>; where high permeability is accompanied by low selectivity and vice versa. This constriction experienced by polymeric membrane has motivates researchers for a new class of membrane materials. Among various candidates, inorganic membrane such as zeolite and carbon molecular sieve has demonstrated to surpass the Robeson upper-bound<sup>5</sup>. Besides, high thermal and chemical stability as well as high mechanical strength of inorganic membrane has shown its wide potential. However, fabricating continuous defect-free inorganic membrane is a challenging task. Aside from its brittle structure, high synthesis temperature and a longtime requirement are the drawbacks of inorganic membrane to attract industrial attentions<sup>6, 7</sup>. Recent membrane development has been focused on mixed matrix membrane (MMM), a combination of polymeric

membrane as continuous phase with inorganic particle as disperse phase. MMM are expected to complement both polymeric and inorganic membrane limitations, and resultant new class of membrane. Significant improvement offered by MMM properties are expected with superiority of inorganic particle, while offering ease processability and maintaining moderate processing cost<sup>8-10</sup>. Moreover, excellent gas separation properties of MMM are the main driving force in development of the membrane. Incorporated inorganic particles could improve separation performance by one or more of the following factors, 1) introducing molecular sieving effect, 2) increasing specific membrane-penetrant interaction, 3) increasing membrane free volume through polymer chain disruptions, and 4) increasing polymer chain rigidity<sup>11-14</sup>. The aforementioned factors could either increase permeability while maintaining selectivity or increase selectivity while maintaining permeability, or increase both selectivity and permeability.

The keys factor in developing ideal MMM are high intrinsic properties of MMM materials and good interaction between polymer and filler. For continuous phase, glassy polymers are preferable choice since it is highly selective with moderate gas permeability, while rubbery polymers has low intrinsic selectivity and only excel on gas permeability. Hence, membranes made from polyimide (PI)-derivative and polysulfone (PSf) are commonly employed as the continuous phase<sup>13-17</sup>.

The selection of fillers remains as the heart of MMM development. It is crucial for the filler to have good interaction with the polymer counterpart. Poor polymer-filler compatibility is likely to cause the leads to defective membrane. Formation of un-selective voids, sieve-in-cage morphology, particle agglomeration, polymer rigidification and pore blockage are of common

defects that result from poor polymer-filler interaction. Compared to other classes of fillers, MOFs possess good interaction with polymer matrix due to the presence of their organic ligands<sup>13, 16</sup>. Besides, spectacular intrinsic properties of MOFs such as high surface area, high adsorption capacity, ease of modifications and high affinity towards certain gas favor MOFs as the filler. ZIF-8, a zeolitic structure MOF, shows a good chemical stability against polar and nonpolar solvents<sup>18</sup>, reorientation of its structure at high pressure<sup>19</sup> and high mechanical strength<sup>20</sup>. In addition, previous works on polymer/ZIF-8 have shown promising results for gas separations<sup>16, 21-25</sup>. Most notably was the work by Ordoñez *et al.*<sup>13</sup>, where incorporation of ZIF-8 into Matrimid® has shown a significant improvement with the absence of interfacial defects even at 50wt% filler loading due to the unique properties of ZIF-8. Another spectacular property of ZIF-8 is the controllability of its particle size. By controlling its synthesis parameters or additive concentrations, the particle size of produced ZIF-8 can be attained up to 1 nm<sup>26, 27</sup>. The controllability of its crystal size is of important factor during the fabrication of asymmetric MMM particularly, in order to ensure that the fillers are small enough to be able to reside among the dense, thin selective layer (typically in range of 100-500 nm<sup>28</sup>).

Identifying filler loading necessary to be dispersed into polymer phases is decisive factor in MMM development. Excessive filler loadings would increase the chances for filler to agglomerate and lead to defective membrane. Whereas, low filler loadings are rarely investigated since only negligible improvement can be expected. To date, the incorporation of ZIF-8 particles has primarily been subjected to the preparation of dense MMMs, whereas studies on asymmetric ZIF 8 MMMs are rarely investigated. Thus, this study aims to develop ideal asymmetric PSf/ZIF-8 membrane with improved CO<sub>2</sub> permeance and CO<sub>2</sub>/CH<sub>4</sub> selectivity by utilizing

relatively low ZIF-8 loadings. In this study, ZIF-8 was synthesized using an aqueous room temperature media with a base-type additive and characterized by means of X-Ray diffraction (XRD), thermal gravimetric analysis (TGA), nitrogen physisorption analysis and transmission electron microscopy (TEM). The MMMs were prepared by varying ZIF-8 incorporation in continuous PSf polymer phase were prepared using dry/wet phase inversion. The influences of ZIF-8 loading on the membrane properties were examined via XRD, TGA, differential scanning calorimeter (DSC) and scanning electron microscopy (SEM). The performances of the MMMs were further evaluated by pure CO<sub>2</sub> and CH<sub>4</sub> gas permeation studies. Experimental results of using prepared ZIF-8 MMMs were compared to that of values reported in the literature.

## 2 Experiment

### 2.1 Materials

Zinc nitrate hexahydrate (Zn(NO<sub>3</sub>)<sub>2</sub>·6H<sub>2</sub>O) was purchased from Alfa Aesar. 2-methylimidazole (H-MeIM), n-hexane, polydimethylsiloxane (PDMS) and triethylamine (TEA) were obtained from Sigma Aldrich. Polysulfone (PSfUdel® P-1700) with density of 1.24 g/cm<sup>3</sup> was procured from Solvay Plastic. *N,N*-methylpyrrolidone (NMP), tetrahydrofurane (THF) and ethanol were purchased from Merck. All chemicals were used without further purification.

### 2.2 ZIF-8 Synthesis

ZIF-8 was prepared by following the same procedure as described in the previous study<sup>29</sup> with the ratio of Zn(NO<sub>3</sub>)<sub>2</sub>:2-MeIM:H<sub>2</sub>O 1:6:500. Briefly, metal salt solution was prepared by

dissolving 2g of  $\text{Zn}(\text{NO}_3)_2 \cdot 6\text{H}_2\text{O}$  (6.72 mmol) in 12.11g of deionized water (20% of total deionized water). For ligand solution, 2-MeIM (3.312g, 40.34 mmol) was dissolved into 48.45g of deionized water and subsequently 3.0 mL of TEA was added. The metal salt solution was gently added to the ligand solution, resulting in a cloudy solution mixture. The solution was stirred vigorously for 30 minutes, followed by centrifugation of the reaction product. The obtained product was washed several times with deionized water to remove excess reactants and subsequently dried in an oven at 60°C for 12 hours. The collected powder was ground into fine particles before further dried in an oven at 100°C for minimum of 12 hours to further evacuate the guest molecules in the ZIF-8 pores.

### 2.3 Membrane Preparation

Asymmetric flat sheet MMM was prepared from solution consist of PSf (25 wt%) in NMP (60 wt%) and THF (15 wt%). The ZIF-8 loading was determined by the total solids percentage as follows.

$$\text{Filler loading (\%)} = \frac{\text{Mass of filler (g)}}{\text{Mass of filler (g)} + \text{Mass of polymer (g)}} \times 100\% \quad (1)$$

Initially, polymer pellet was dried in an oven at 60°C while as-synthesized ZIF-8 was dried at 100°C for at least 12 hours to remove trapped water. The precalculated amount of ZIF-8 (**Table 1**) was added to NMP-THF solvent and sonicated for 2 hours to uniformly disperse the ZIF-8 in the solvent. Approximately 10 wt% of the polymer pellets were then added to the ZIF-8

suspension as “priming” procedure. The mixture was kept stirred until all the polymer pellets dissolved before remaining polymer pellets were gradually added and dissolved. The solution was left standing for overnight to check solution homogeneity. The solution was then cast on a clean glass plate using a casting bar at an ambient atmosphere to a thickness of 120-190  $\mu\text{m}$ . The cast film remained free standing in the atmosphere for a certain period before being immersed in water at room temperature, where the membrane peeled off the glass plate spontaneously. After the membrane was kept immersed in water for 1 day, the membrane was solvent-exchanged by immersing in methanol for 2 h, followed by immersion in n-hexane for 2 h and then air-dried for 24 hours. The asymmetric flat sheet pristine PSf membrane was prepared by the same process as described for MMM without ZIF-8 incorporation. The surface of the prepared membranes was contacted with 3wt% PDMS/n-hexane solution for 10 min to seal possible pinholes. Then, the membrane underwent “curing” at 60°C for approximately 12 h.

**Table 1.** The amount of ZIF-8 loading into the PSf matrix

<b>Sample abbreviation</b>	<b>ZIF-8 loading (wt% total solids)</b>	<b>Glass transitional temperature, <math>T_g</math> (°C)</b>
Neat	0	184.7
M0.25	0.25	174.9
M0.5	0.5	175.0
M0.75	0.75	170.2
M1.0	1.0	170.2
M3.0	3.0	167.7
M5.0	5.0	173.4
M7.0	7.0	172.0
M10.0	10.0	167.7

## 2.4 Characterizations

Differential scanning calorimeter (DSC, Mettler Toledo DSC 822e) was used to determine the glass transition temperature ( $T_g$ ) of the prepared membranes. The membrane sample was cut into small pieces, weighed and placed into pre-weighed aluminium crucible. Then, the sample was heated from 50 to 400°C at a heating rate of 10°C min<sup>-1</sup> in the first cycle to remove the thermal history and subsequently cooled from 400 to 30°C at a heating rate of 10°C min<sup>-1</sup>. The same heating protocol was repeated in the next heating cycle.  $T_g$  of the sample was determined as the midpoint temperature of the transition region in the second heating cycle.

Thermogravimetric analysis (TGA) was used to characterize thermal stability of the prepared ZIF-8 and MMM samples. TGA records the weight changes of sample when heated continuously. The samples were heated from 50 to 900°C at the heating rate of 10°C min<sup>-1</sup> under nitrogen atmosphere with a nitrogen flow rate of 20 mL min<sup>-1</sup>.

The specific surface area of the ZIF-8 crystal was measured by using Micromeritics gas adsorption analyzer ASAP2010 instruments equipped with commercial software of calculation and analysis. The BET surface area was calculated from the adsorption isotherms using the standard Brunauer–Emmett–Teller (BET) equation. The micropore volume was obtained using the t-plot method of the Lippens and de Boer to the adsorption data.

X-Ray Diffraction (XRD) analysis was carried out using Siemens D5000 Diffractometer to measure the crystallinity of ZIF-8 and MMM samples. Scanning range of  $2\theta$  between 5° and 40° were employed with copper K $\alpha$  ( $\lambda = 0.1541$  nm at 40 kV and 30 mA) was used as the source of radiation

Transmission electron microscope (TEM) (JEOL, JSM-6701FJEOL 1230) was applied to observe the macrostructures of the ZIF-8. Samples were prepared by dispersing ZIF-8 powder into methanol. A drop of methanol was used for the dispersion of ZIF-8 on carbon-coated copper grids operating at 300 kV.

Scanning electron microscopy (SEM) was used to observe the membrane structure and morphology. Membrane samples were fractured cryogenically in liquid nitrogen. The samples were coated with gold before they were imaged and photographed by employing a scanning electron microscope (TM3000, Hitachi) equipped with an energy dispersive X-ray spectrometer (EDX) (XFlash® 430H Detector, Bruker).

Tensile strength and elongation at break of the membranes were evaluated according to the ASTM D3039 standard by using an LRX 2.5 SKN Llyod Instrument. Membranes were cut into 5 cm long and placed in the equipment.

## 2.5 Gas Permeation

Gas permeation tests were performed using a constant pressure variable volume system described elsewhere<sup>30</sup>. The membranes were placed into the permeation cell with an effective permeation area of 13.5 cm<sup>2</sup> and exposed to pure CH<sub>4</sub> and CO<sub>2</sub>, respectively. Feed pressure was controlled at 4 bar at temperature 27°C. Pressure-normalized flux (permeance, cm<sup>3</sup> (STP)/cm<sup>2</sup> s cmHg) of gas *i* was calculated as follows:

$$\left(\frac{P_i}{l}\right) = \frac{1}{A\Delta p} \times \frac{dV_i}{dt} \quad (2)$$

Where  $i$  represents the gas penetrant  $i$ ,  $V_i$  is the volume of gas permeated through the membrane ( $\text{cm}^3$ , STP),  $A$  the effective membrane area ( $13.5 \text{ cm}^2$ ),  $t$  the permeation time (s) and  $\Delta p$  is the transmembrane pressure drop (cmHg). Selectivity was obtained using Eq. (3):

$$\alpha_{i/j} = \frac{(P_i/l)}{(P_j/l)} \quad (3)$$

Where  $\alpha_{i/j}$  is the selectivity of gas penetrant  $i$  over gas penetrant  $j$ ,  $P_i/l$  and  $P_j/l$  are the permeance of gas penetrant  $i$  and  $j$ , respectively.

### 3 Result and Discussion

#### 3.1 ZIF-8 Characterizations

The X-Ray diffractogram of the prepared ZIF-8 and MMM are illustrated in **Figure 1**. The XRD pattern of prepared ZIF-8 shows strong peaks appeared at  $2\theta = 7.30, 10.35, 12.70, 14.80, 16.40$  and  $18.00$ , which correspond to the planes  $\{110\}$ ,  $\{200\}$ ,  $\{211\}$ ,  $\{220\}$ ,  $\{310\}$ , and  $\{222\}$ , respectively. This pattern is in good agreement with literature<sup>31</sup>, therefore confirmed the formation of pure phase ZIF-8. The  $\text{N}_2$  sorption of the ZIF-8 shows type-I isotherm, indicating permanent microporosity with no hysteresis loop (**Figure 1b**). The first steep increase at relatively low pressure ( $p/p_0 < 0.1$ ) reveals the microporosity and the second steep increase at relatively high pressure ( $p/p_0 > 0.9$ ) indicates the textural meso/macroporosity of the crystal. The BET surface area, micropore volume and liquid density of ZIF-8 are  $1032 \text{ m}^2/\text{g}$ ,  $0.3 \text{ cm}^3/\text{g}$  and

0.8086 g/cm<sup>3</sup>, respectively, which is comparable to the ZIF-8 synthesized at room temperature using aqueous media<sup>31</sup> (Table 2). Figure 2 represents the TEM images of the ZIF-8. The prepared ZIF-8 possesses rhombic dodecahedron morphology; showing a good agreement with literature<sup>32</sup>. The particle size of prepared samples was estimated using the TEM images and the values are tabulated in Table 2.

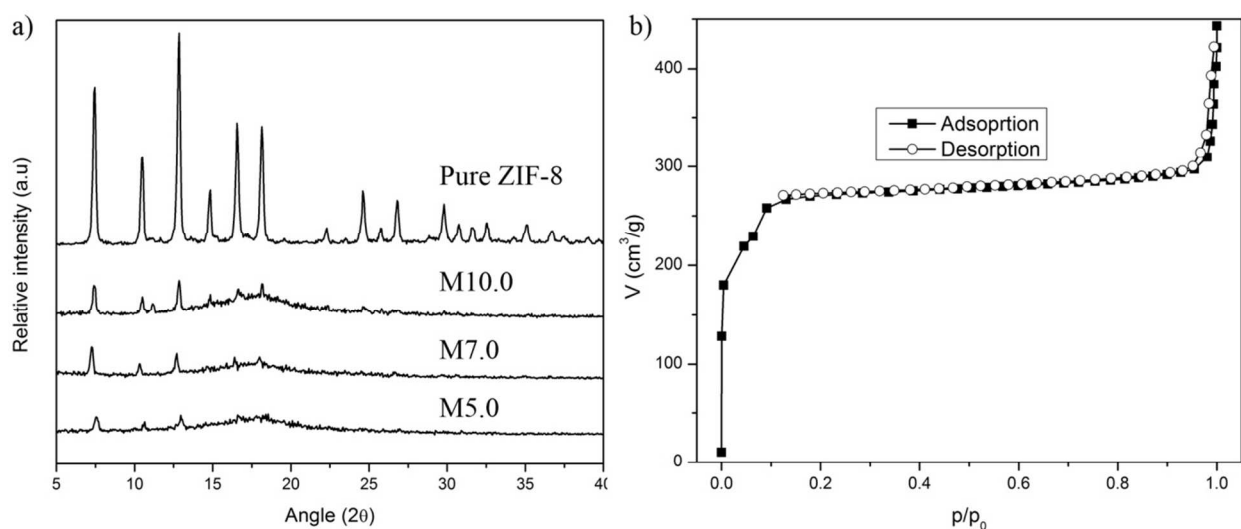


**Figure 1.** a) X-ray diffraction pattern of MMM at loading of 5.0, 7.0, and 10.0wt% (total solids) with pure ZIF-8. (b) N<sub>2</sub> sorption isotherm of prepared ZIF-8

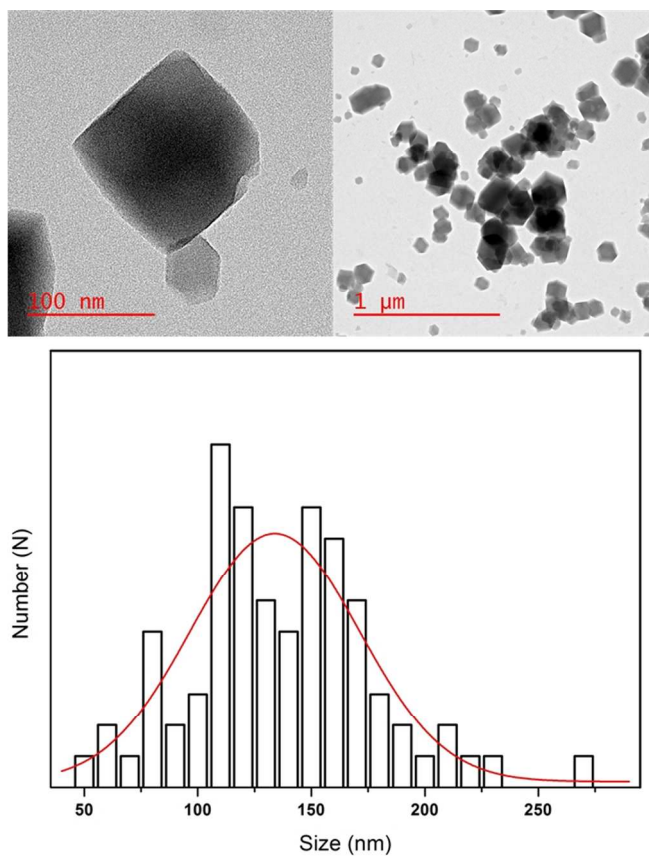


**Figure 2.** Morphology and particle size distribution of prepared ZIF-8. The red line represents the Gaussian fit.

**Table 2:** Surface properties of ZIF-8 synthesized in an aqueous room temperature

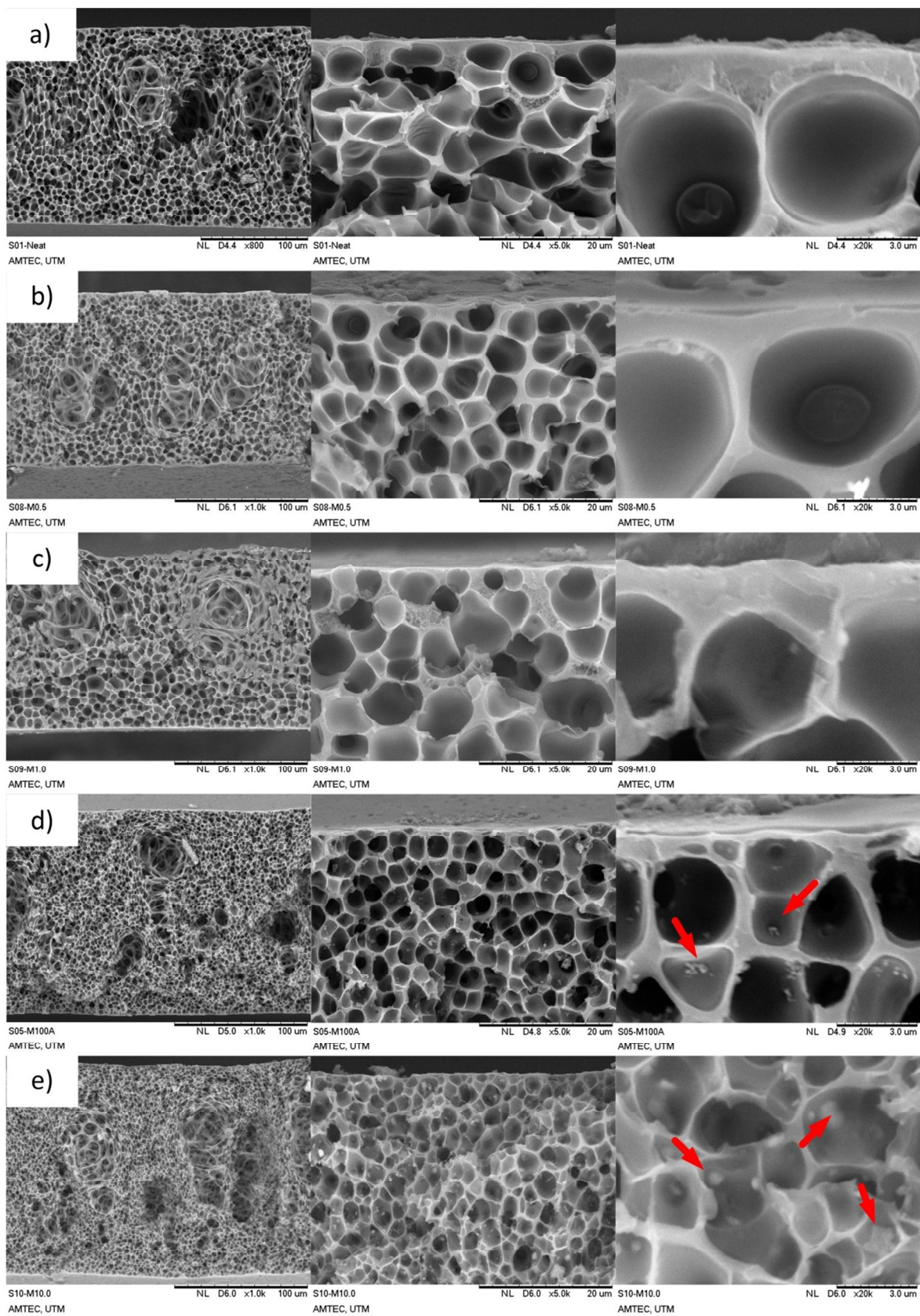
ZIF-8	Particle size (nm)	BET surface area (m <sup>2</sup> /g)	Microporous volume (cm <sup>3</sup> /g)
32	~85	1079	0.31
31	~60	811	0.32
This work	~134	1032	0.30

### 3.2 Membrane Characterization

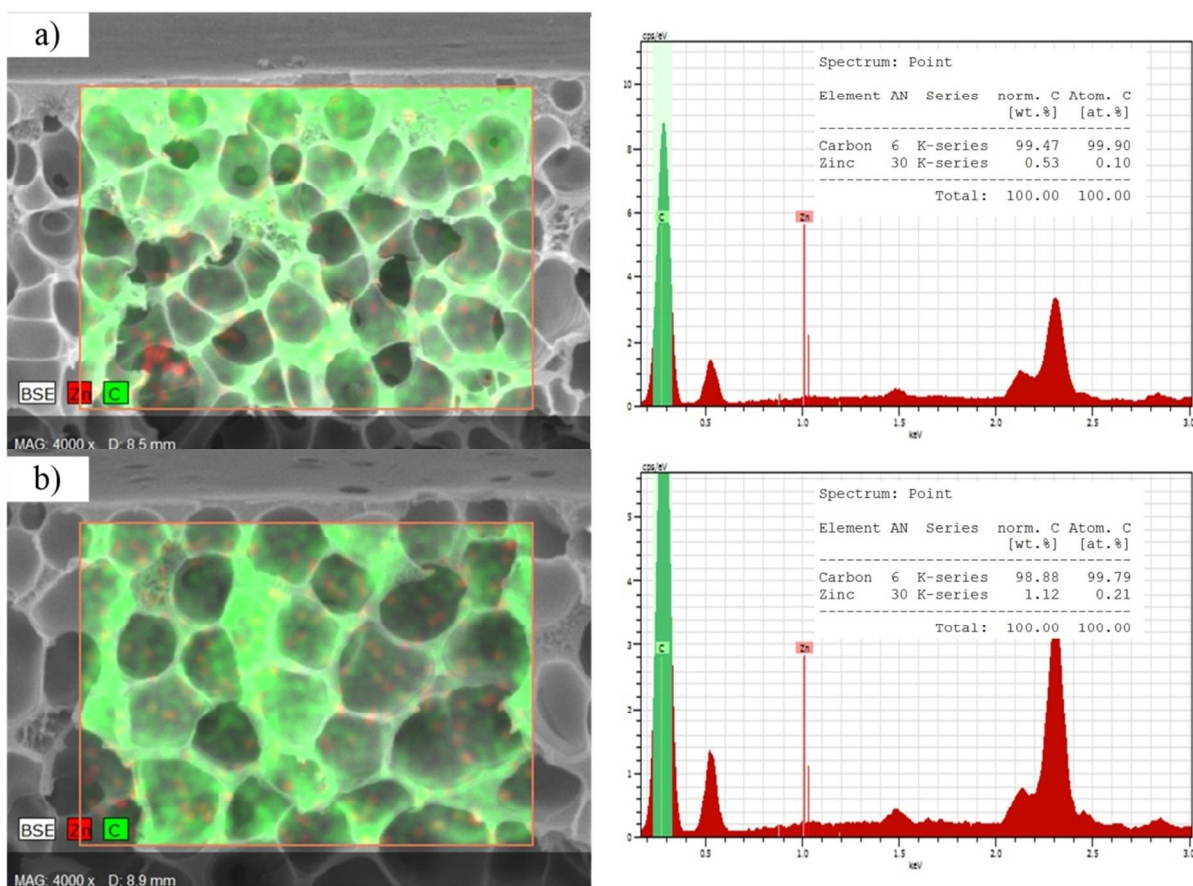
The XRD peak of MMM aims to identify structural changes of ZIF-8 after being incorporated into PSf matrix. However, the ZIF-8 peaks were not observed when filler loading was < 3wt% of total solid since the peaks of ZIF-were clouded by the PSf matrix (not included in this study). The ZIF-8 peaks within MMM could be observed at 5wt% and higher loading (**Figure 1a**). This implies that there were no changes in the ZIF-8 structure even after undergoing the continuous membrane preparation procedure. Since similar membrane preparation procedure was implemented throughout the study, it is fair to assume that incorporated ZIF-8 was able to sustain its structure at different loadings.

Cross-sectional morphologies of prepared membranes are presented in **Figure 3**. A common asymmetric structure could be clearly observed for neat PSf membrane with an apparent active layer accompanied by a sponge-like substructure (**Figure 3a**). The dry phase inversion was introduced to form a thin-selective layer through evaporation of volatile solvent (THF). The sponge-like substructure was also observed as a result of the solvent exchange between NMP and water during the wet inversion. Similar cross-sectional morphology was also observed for all prepared MMMs due to the same fabrication protocol. At low ZIF-8 loading, the overall morphology of prepared membranes seems to remain intact. The presence of ZIF-8 particles were not visible for filler loading <1wt% of total solids (**Figure 3b, c**) indicating the absence of ZIF-8 agglomeration. The low ZIF-8 loading MMMs were further analyzed by energy dispersed x-ray spectrometer (EDX) analysis. The EDX analysis of M0.5 (**Figure 4a**) and M1.0 (**Figure 4b**) revealed the presence of Zn element which represent the ZIF-8 particles. Moreover, Zn

element well scattered throughout the membrane indicates that the ZIF-8 particles were uniformly distributed. At high ZIF-8 loading, large aggregations of ZIF-8 particles were clearly visible (red arrows in **Figure 3d,e**) throughout the sponge-like structure of the membranes with cluster size estimated around ~300nm for M5.0 and ~500nm for M10.0. Nanoparticles tend to form a bigger cluster due to interaction between their surfaces, especially when a large number of the particles are incorporated. It was also observed that the sponge-like substructure of the membrane became more compact when ZIF-8 loading was as high as 5wt% and 10wt%, indicating the reduced solvent-nonsolvent exchange rate.



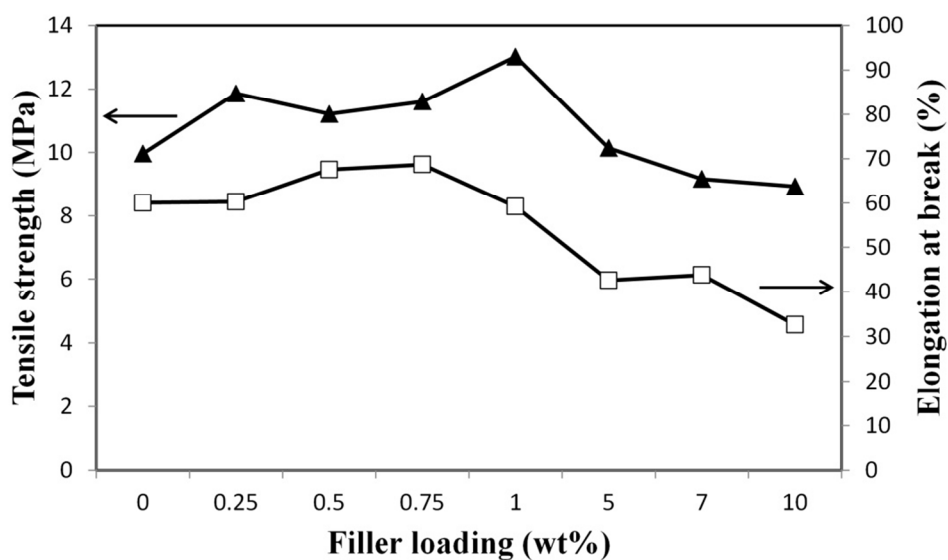
**Figure 3.** SEM images (Left – 1000 $\times$ , middle – 5000 $\times$ , and right – 20,000 $\times$ ) of cross sectional morphologies of membranes made of different ZIF-8 loadings, a) 0wt%, b) 0.5wt%, c) 1.0wt%, d) 5.0wt%, and e) 10.0wt%. Red arrows represent the agglomeration of ZIF-8 particles within the porous substructure.



**Figure 4.** EDX analysis of cross sectional morphology of a) M0.5, and b) M1.0. The element Zn (red dot) represents the ZIF-8 particle in membrane

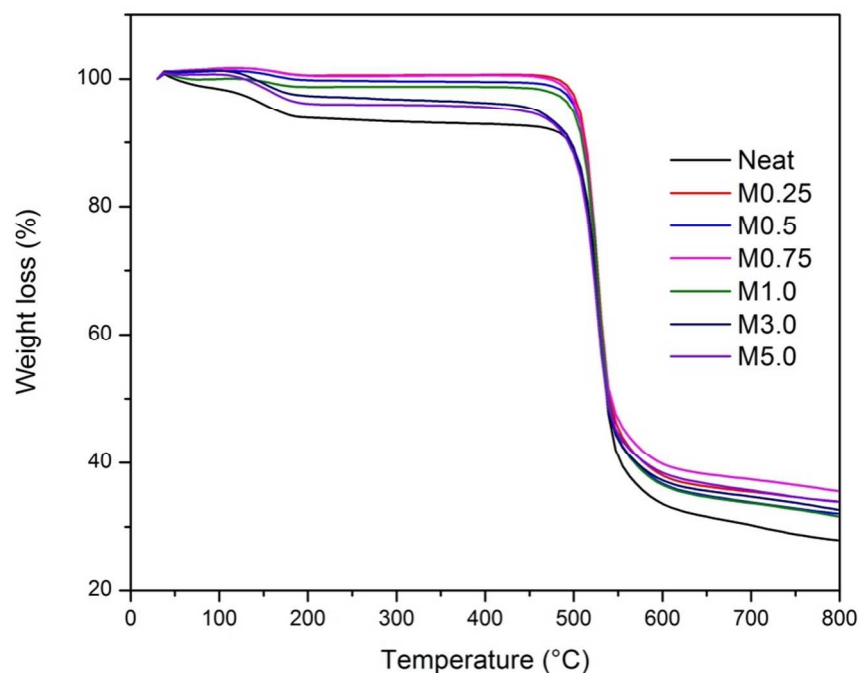
Mechanical stability of the prepared membranes was measured and the data are presented in **Figure 5**. It is seen that the tensile strength increased with the increment of filler loadings up to

1wt% ZIF-8. Similarly, the elongation at break has also been observed to be enhanced upon the addition of filler loadings up to 0.75wt%. It is speculated that ZIF-8 can be easily interacted with PSf matrix to improve the tensile strength of the prepared membranes at low filler loadings. Additionally, a good dispersion of ZIF-8 within the PSf matrix may disrupt the polymer chains, leading to more flexible membrane. At a higher filler loading of more than 1 wt%, the tensile strength has been observed to be gradually decreased. The elongation in break was also decreased upon the addition of filler loadings of above 0.75 wt%. Khare and Burris<sup>33</sup> reported that when particles in polymer composite began to agglomerate, the stress induced are directed towards the agglomeration and resulting the deterioration of its mechanical properties. This behavior does explain the sudden drop in mechanical properties of the MMMs as ZIF-8 loading exceeding 0.75wt%. Evidently, the severe ZIF-8 agglomeration suffered by M10.0 (**Figure 3e**) demonstrated to have poor mechanical properties compared to lower ZIF-8 loadings. These results are in good agreement with previously reported MOF-based MMM<sup>13, 16, 34</sup>.



**Figure 5.** Tensile strength and elongation at break of the prepared membranes

Thermal stability of the prepared membranes is presented in **Figure 6**. Neat membrane experienced the first weight loss (%) at temperature around 100°C, which was attributed to the presence of water trapped in the membrane during the wet phase inversion. On contrary, MMMs demonstrates insignificant weight loss due to the hydrophobic nature of ZIF-8 that minimized water trap within the membrane<sup>35</sup>. Second weight loss at approximately 500°C was attributed to the degradation of polymer matrix. No significant difference between thermal stability of neat membrane and MMMs was observed, which suggested that ZIF-8 loading <5wt% of total solids did not seriously affect the overall thermal stability of the prepared membranes.

**Figure 6.** TGA curves of prepared membranes

The  $T_g$  values of the prepared membranes are summarized in **Table 1**. The  $T_g$  of the neat PSf membrane is comparable to the previously reported value<sup>36</sup> despite the differences in membrane preparation history. A significant change in  $T_g$  was observed from Neat to M0.25 which indicates that even a small amount of filler (0.25wt%) resulting significant change in membrane properties. The decreased in  $T_g$  indicates the increment of polymer chain flexibility attributed by the ZIF-8 particles that reside among the polymer chains. Further increase in filler loading up to 3.0wt% (M3.0) resulted in further lowering  $T_g$ . An increase in  $T_g$  for M5.0 and M7.0 was likely induced by severe agglomeration at the high ZIF-8 loading that reduced the filler-polymer interaction. Sudden drop in tensile strength at high filler loading (**Figure 5**) corroborate the change of  $T_g$ .

### 3.3 Gas Permeation Test

The ideal CO<sub>2</sub>/CH<sub>4</sub> separation performance of all prepared membranes is presented in **Table 3**. The CO<sub>2</sub> permeance of the neat PSf membrane in **Table 3** is lower than the value of previously reported, which is due to the difference in solvent, polymer concentration and fabrication history<sup>15, 30, 37</sup>.

**Table 3.** Effect of ZIF-8 loading on CO<sub>2</sub> and CH<sub>4</sub> permeance through PSf/ZIF-8 MMMs

Sample	ZIF-8 Loading	Permeance (GPU) <sup>a</sup>		Ideal CO <sub>2</sub> /CH <sub>4</sub> Selectivity <sup>b</sup>
		CO <sub>2</sub>	CH <sub>4</sub>	
Neat	0	21.27 ± 6.35	1.33 ± 0.35	19.43
M 0.25	0.25	25.47 ± 7.82	1.31 ± 0.51	20.28
M 0.5	0.5	29.22 ± 3.68	1.26 ± 0.05	23.16

M 0.75	0.75	33.35 ± 3.46	3.45 ± 0.35	9.66
M 1.0	1	31.42 ± 0.15	2.32 ± 0.06	13.55
M 3.0	3	25.16 ± 4.39	1.70 ± 0.28	14.83
M 5.0	5	15.70 ± 0.79	0.55 ± 0.07	28.50
M 7.0	7	16.01 ± 2.28	1.99 ± 0.71	8.01
M 10.0	10	22.71 ± 4.99	2.85 ± 0.59	7.97

---

<sup>a</sup> GPU =  $1 \times 10^{-6} \text{ cm}^3 \text{ cm}^{-2} \text{ s}^{-1} \text{ cmHg}^{-1}$

<sup>b</sup>The ideal selectivity presented is based on average of membrane modules tested, and not necessary equal to the ratio of average permeance

± Represent the standard deviation

Generally, uniformly dispersed fillers in the polymer matrix disrupt polymer chain packing, which induces excess free volume and boost gas permeation with insignificant changes in gas pair selectivity<sup>11-14, 38</sup>. Upon incorporating 0.25wt% ZIF-8, only small changes in both permeance and selectivity were observed thus suggesting that minimal loading of ZIF-8 particles shows insignificant impact on the overall membrane properties.

At ZIF-8 loading of 0.5wt%, CO<sub>2</sub> permeance increased and CH<sub>4</sub> permeance decreased. If disruption of polymer chain were the only reason for the changes in gas permeation, permeances of both CO<sub>2</sub> and CH<sub>4</sub> should be equally enhanced. Therefore, there should be some other factors to distinguish the transport of CO<sub>2</sub> and CH<sub>4</sub>. The increase in CO<sub>2</sub> permeance could be resulted from the electrostatic field of ZIF-8 with quadrupole moment of CO<sub>2</sub>, while having no specific interaction with CH<sub>4</sub><sup>16, 39, 40</sup>. Hence, the incorporated ZIF-8 at 0.5wt% loading contributed to the substantial increase (19%) in the CO<sub>2</sub>/CH<sub>4</sub> selectivity. Although it was reported that molecular sieving of ZIF-8 also contribute in CO<sub>2</sub>/CH<sub>4</sub> separation<sup>13</sup>, we speculated that the effect only

plays as minor role in improving the membrane selectivity due to flexibility of ZIF-8 structure that accessible by larger molecules<sup>41</sup>.

Increasing trend of CO<sub>2</sub> permeance was continued as the filler loading increased to 0.75wt%, consistent with the disruption in polymer packing that facilitates the gas permeation. However, increase in CH<sub>4</sub> permeance surpassed CO<sub>2</sub> permeance, thus diminishing the gas pair selectivity below that of the neat PSf membrane. This suggests the formation of unselective voids between the filler and polymer matrix. Further increase in ZIF-8 loading consistently resulted in gas pair selectivity below the neat PSf membrane until the loading reached 5wt%.

The permeance for 5wt% ZIF-8 showed 58% decrease from the neat PSf membrane for CH<sub>4</sub>, while only 38% decrease for CO<sub>2</sub>. Consequently, the resultant ideal CO<sub>2</sub>/CH<sub>4</sub> selectivity of 28.5 is 47% higher than the neat PSf membrane. Similar trend was also reported by Li *et al.*<sup>42</sup> when utilizing nano ZIF-7 within dense poly(etherblock-amide) membrane. It was reported that gases permeance began to decrease at medium (22wt%) and high (34wt%) loading of ZIF-7 due to restricted polymer chain and higher gas pair selectivity is achieved. At high filler loading increase in the distance of tortuous permeation path overwhelmed the access of permeate gases to ZIF-8 pores<sup>13</sup>. This trend is consistent with the decrease in elongation at break caused by the restricted motion of polymer chains<sup>43</sup>. Consequently, mass transport resistance increased significantly for both CO<sub>2</sub> and CH<sub>4</sub>, resulting in significant decrease in permeances of both gases. Moreover, the CH<sub>4</sub> permeance is more affected by restricted polymer chain due to larger kinetic molecular diameter and this leads to ideal CO<sub>2</sub>/CH<sub>4</sub> selectivity to be increased considerably.

At higher ZIF-8 loading of 7wt% and 10wt%, severe deterioration in the membrane performance was observed. Inaccessible ZIF-8 pores within the formed clusters have limited the interaction and thus diminished both CO<sub>2</sub> permeance and ideal CO<sub>2</sub>/CH<sub>4</sub> selectivity at 7wt% ZIF-8. Further increase in the loading created clusters that were larger than the thickness of the dense selective layer would form at high filler loading. Spaces between the clusters would act as unselective channels crossing the dense layer that are accessible for both gases to permeate easily<sup>44</sup>. Hence, gas pair selectivity diminished severely, accompanied by higher gas permeances at 10wt%. The gas permeation behavior, changing from low to high ZIF-8 loading, is illustrated schematically in **Figure 7** for better understanding.

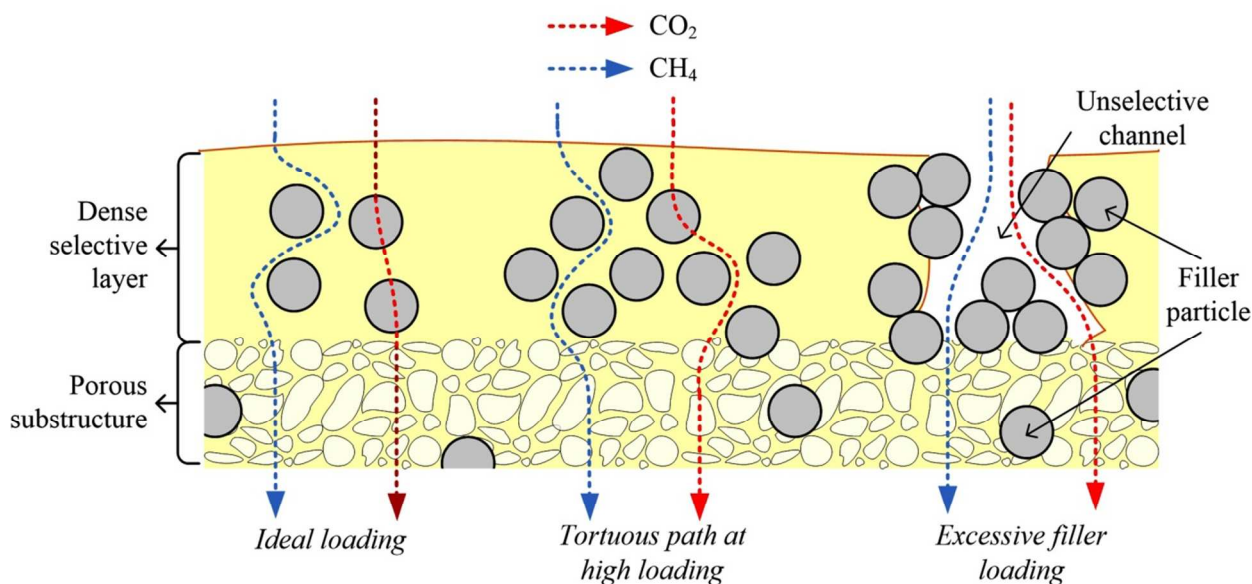


**Figure 7.** Illustration of gas permeation across different ZIF-8 loading in asymmetric membrane

The influences of filler loading on membrane morphology are further evaluated through its gas separation performance. According to Hashemifard *et al.*<sup>44</sup>, the plots of MMM's CO<sub>2</sub>

permeance versus ideal CO<sub>2</sub>/CH<sub>4</sub> selectivity, both normalized by those of the host polymeric membrane, are classified into; case 1 (ideal morphology), case 2 (unselective voids), case 3 (polymer chain rigidification/partial pore blockage), and case 4 (filler pore blockage). Ideal morphology represents increase both in CO<sub>2</sub> permeance and CO<sub>2</sub>/CH<sub>4</sub> selectivity, unselective voids increase in CO<sub>2</sub> permeance and decrease in gas pair selectivity, filler pore blockage decrease both in permeance and selectivity, and polymer rigidification and/or partial pore blockage decrease in permeance and increase in gas pair selectivity.

**Figure 8** shows the plots for the MMMs fabricated in this work. According to the figure, M0.25 membrane does not show any significant impact on gas separation performance. M0.5 membrane is classified as ideal morphology MMM. Above 0.5wt% of ZIF-8 loading, none of the MMMs were classified as ideal morphology despite the presence of the organic ligand in the ZIF-8 particles, which would minimize interfacial defects. Instead, the plots scattered all over within non-ideal cases (case 2, 3 and 4) of the morphological diagram. At this point, the ZIF-8 particles began to agglomerate, as evident via SEM images (**Figure 3**) and mechanical properties (**Figure 5**). Increasing ZIF-8 loading prompt larger filler cluster to forms and eventually punctured the selective layer, causing severe membrane properties and performances deterioration. Similar results were also reported by Wahab *et al.*<sup>17</sup> when incorporating 0.1wt%, 1wt% and 10wt% nanoscale silica spheres into PSf matrix of asymmetric MMM. The inter-particle attractive forces tend to create particle aggregation especially at high filler loading, which causes severe cluster formation and deteriorate the membrane performance. Moreover, delayed solvent-nonsolvent exchange rate after increasing ZIF-8 loading (**Figure 3**) that caused tightening of polymer chain may influence the integrity of selective layer formation since similar

membrane preparation was used. Hence, these two factors have caused the fluctuation in membrane performance without distinctive permeation behavior after ZIF-8 embodied exceeding the ideal loading and scattered in non-ideal cases.

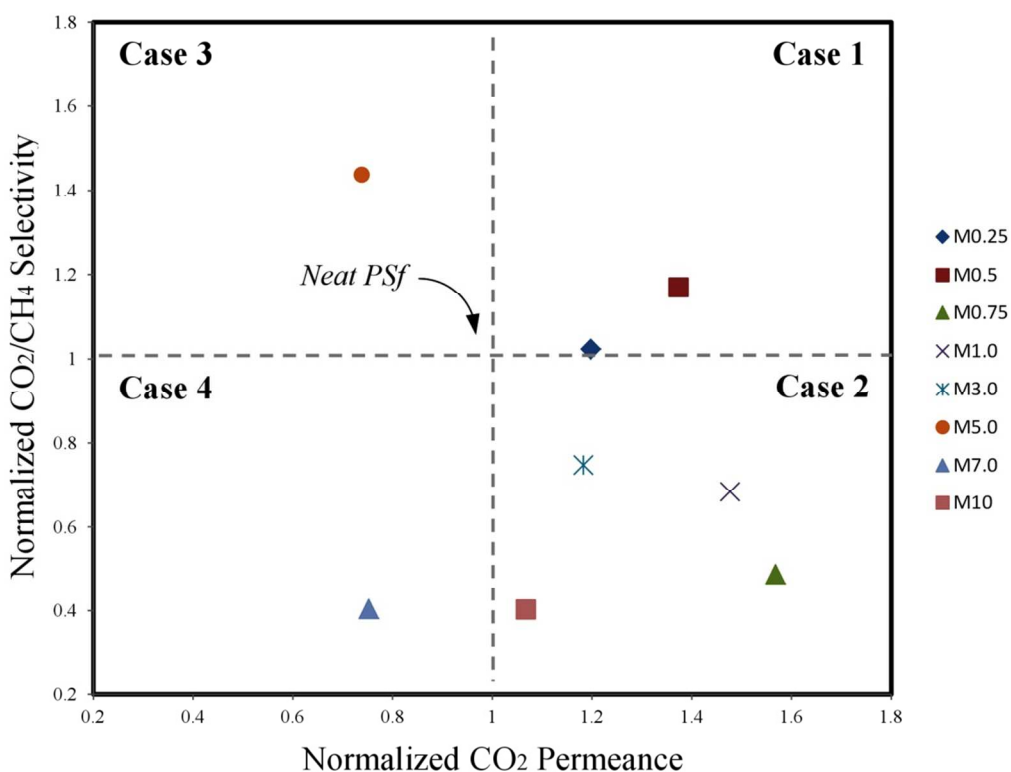


**Figure 8.** Morphological diagram of prepared PSf/ZIF-8 MMMs

### 3.4 Comparison with literature

The influence of ZIF-8 on gas separation of MMM are often described as 1) enhancement of CO<sub>2</sub> diffusivity coefficient through polymer chain disruption exceeding CH<sub>4</sub><sup>45</sup>; 2) interaction between quadrupole moment of CO<sub>2</sub> with the weak electrostatic field of ZIF-8<sup>16</sup>; and/or 3)

molecular sieving induced by ZIF-8<sup>13</sup>. The presence of ZIF-8 within polymeric phase were expected to produce an ideal MMM when dispersed in PPEES<sup>21, 22</sup> and Matrimid®<sup>16</sup>. However, embodying ZIF-8 into polymer matrix does not necessarily lead to ideal MMMs. There were also reports that the CO<sub>2</sub> separation performance of ZIF-8-based MMMs scattered within Case 2 domain (due to highly permeable and poor intrinsic CO<sub>2</sub>/CH<sub>4</sub> selectivity of pure ZIF-8)<sup>24, 25</sup> and Case 3 domain (rigidified chain that restrict permeation of both CO<sub>2</sub> and CH<sub>4</sub>)<sup>13, 23</sup>. However, direct comparison between this work with literatures are quite challenging as the different investigated parameters such as ZIF-8 properties, filler loading, membrane materials and configurations, and operating conditions were involved. Therefore, CO<sub>2</sub> permeance and CO<sub>2</sub>/CH<sub>4</sub> selectivity of MMMs normalized to the continuous polymeric phase were employed for comparison (**Table 4**).

While majority of ZIF-8-based MMMs were prepared as dense membranes, this study focused on asymmetric PSf/ZIF-8 membranes since it is more relevant to practical applications. The performance of M0.5 membrane is superior as compared to neat counterpart with improvement in CO<sub>2</sub> permeance and CO<sub>2</sub>/CH<sub>4</sub> selectivity by 37% and 19%, respectively. These results fall within the ideal MMM range, while exceeding the ideal loading leads to deterioration of membrane performance. The ideal loading of this study was significantly smaller compared to literatures, where higher loading of ZIF-8 were embodied without the presence of defective behavior<sup>16, 21, 22</sup>. It seems that this challenge is exclusive for asymmetric membrane which thin selective layer can only accommodate limited amount of filler before creating unselective channel across the layer, while dense membrane is able to withstand higher loading without deterioration<sup>44</sup>. Moreover, despite comparatively low ZIF-8 loading, improvements of both CO<sub>2</sub>

permeance and ideal CO<sub>2</sub>/CH<sub>4</sub> selectivity are comparable with other ZIF-8-based MMM that utilized higher filler loading. It can be speculated that even the amount of the ZIF-8 is small, its volume fraction resides within the thin selective layer can be as high as in the dense membrane to provide substantial improvement in membrane performances.

**Table 4.** Comparison between polymer/ZIF-8

Polymer	ZIF-8 size (nm)	Membrane configuration	Loading (wt% total solids)	Normalized CO <sub>2</sub> permeability*	Normalized $\alpha_{\text{CO}_2/\text{CH}_4}$ *	Reference
Matrimid	~100	Dense	50	0.459	2.865	13
PPEES	~500	Dense	10	1.393	1.290	21, 22
Matrimid	~500	Dense	30	3.188	1.147	16
		Asymmetric	30	2.2 <sup>m</sup>	1.267 <sup>m</sup>	16
PEBAX	~500	Dense	30	1.489	0.757	24
PMPS	~50	Dense	8.3	2.712	0.880	25
PIM-1	~50	Dense	28 <sup>v</sup>	0.973	1.310	23
PSf	~100	Asymmetric	0.5	1.374	1.192	This work

<sup>v</sup> volumetric percent

\* values were obtained by normalized MMM respective to neat membrane

<sup>m</sup> mixed gas permeation using 75vol% CO<sub>2</sub> in CH<sub>4</sub>

#### 4 Conclusion

This study focuses on the CO<sub>2</sub> and CH<sub>4</sub> permeation behavior of asymmetric PSf/ZIF-8 MMMs with various ZIF-8 loadings. Indefinite trend was observed between the gas permeation and ZIF-8 loadings. The ideal ZIF-8 loading of 0.5wt% demonstrated most promising result with improvement in CO<sub>2</sub>/CH<sub>4</sub> separation originated mainly from specific interaction between

electrostatic fields of ZIF-8 with quadrupole moment of CO<sub>2</sub>. Moreover, overall mechanical stability of the resulted MMM also improved due to good dispersion of ZIF-8 in PSf matrix. Insignificant change on CO<sub>2</sub>/CH<sub>4</sub> separation properties at lower ZIF-8 loading (0.25wt%) due to limited filler availability, while excessive ZIF-8 loading provoke particles to agglomerates and deteriorate membrane performance.

Compared to dense polymer/ZIF-8 membranes reported in literatures, the ideal ZIF-8 loading of asymmetric PSf/ZIF-8 prepared in this study was significantly smaller. This problem seems unique for the asymmetric membrane since the selective layer is very thin, typical around 100 – 500 nm, and can accommodate only limited amount of ZIF-8. Moreover, ZIF-8 particles also observed within the porous support do not contribute to gas separation. Since the asymmetric membranes are more relevant in practical applications, this issue should be seriously addressed in future research on asymmetric MMMs for gas separation.

### **Acknowledgement**

The authors gratefully acknowledge the Ministry of Education (MOE) for the scholarship and Long-Term Research Grant Scheme (LRGS) Program under Universiti Teknologi Malaysia with the grant number Q.J130000.2452.04H71

## References

1. R. W. Baker and K. Lokhandwala, *Industrial & Engineering Chemistry Research*, 2008, 47, 2109-2121.
2. S. Loeb, 1981, 153, 1-9.
3. S. P. Nunes and K. V. Peinemann, in *Membrane Technology*, Wiley-VCH Verlag GmbH & Co. KGaA, 2006, pp. 53-90.
4. L. M. Robeson, *Journal of Membrane Science*, 2008, 320, 390-400.
5. K. Hunger, N. Schmeling, H. B. T. Jeazet, C. Janiak, C. Staudt and K. Kleinermanns, *Membranes*, 2012, 2, 727-763.
6. S. Battersby, T. Tasaki, S. Smart, B. Ladewig, S. Liu, M. C. Duke, V. Rudolph and J. C. Diniz da Costa, *Journal of Membrane Science*, 2009, 329, 91-98.
7. K. Sato, K. Sugimoto, Y. Sekine, M. Takada, M. Matsukata and T. Nakane, *Microporous and Mesoporous Materials*, 2007, 101, 312-318.
8. T.-S. Chung, L. Y. Jiang, Y. Li and S. Kulprathipanja, *Progress in Polymer Science*, 2007, 32, 483-507.
9. M. A. Aroon, A. F. Ismail, T. Matsuura and M. M. Montazer-Rahmati, *Separation and Purification Technology*, 2010, 75, 229-242.
10. P. S. Goh, A. F. Ismail, S. M. Sanip, B. C. Ng and M. Aziz, *Separation and Purification Technology*, 2011, 81, 243-264.
11. B. Zornoza, C. Téllez and J. Coronas, *Journal of Membrane Science*, 2011, 368, 100-109.
12. L. Ge, Z. Zhu and V. Rudolph, *Separation and Purification Technology*, 2011, 78, 76-82.
13. M. J. C. Ordoñez, K. J. Balkus, J. P. Ferraris and I. H. Musselman, *Journal of Membrane Science*, 2010, 361, 28-37.
14. S. Rafiq, Z. Man, A. Maulud, N. Muhammad and S. Maitra, *Separation and Purification Technology*, 2012, 90, 162-172.
15. B. Zornoza, A. Martinez-Joaristi, P. Serra-Crespo, C. Tellez, J. Coronas, J. Gascon and F. Kapteijn, *Chemical communications*, 2011, 47, 9522-9524.
16. S. Basu, A. Cano-Odena and I. F. J. Vankelecom, *Separation and Purification Technology*, 2011, 81, 31-40.
17. M. F. A. Wahab, A. F. Ismail and S. J. Shilton, *Separation and Purification Technology*, 2012, 86, 41-48.
18. K. S. Park, Z. Ni, A. P. Cote, J. Y. Choi, R. Huang, F. J. Uribe-Romo, H. K. Chae, M. O'Keeffe and O. M. Yaghi, *Proceedings of the National Academy of Sciences of the United States of America*, 2006, 103, 10186-10191.
19. S. A. Moggach, T. D. Bennett and A. K. Cheetham, *Angewandte Chemie*, 2009, 48, 7087-7089.
20. J. C. Tan, T. D. Bennett and A. K. Cheetham, *Proceedings of the National Academy of Sciences*, 2010, 107, 9938-9943.
21. K. Díaz, L. Garrido, M. López-González, L. F. del Castillo and E. Riande, *Macromolecules*, 2010, 43, 316-325.
22. K. Díaz, M. López-González, L. F. del Castillo and E. Riande, *Journal of Membrane Science*, 2011, 383, 206-213.

23. A. F. Bushell, M. P. Attfield, C. R. Mason, P. M. Budd, Y. Yampolskii, L. Starannikova, A. Rebrov, F. Bazzarelli, P. Bernardo, J. Carolus Jansen, M. Lanč, K. Friess, V. Shantarovich, V. Gustov and V. Isaeva, *Journal of Membrane Science*, 2013, 427, 48-62.
24. V. Nafisi and M.-B. Hägg, *Journal of Membrane Science*, 2014, 459, 244-255.
25. L. Diestel, X. L. Liu, Y. S. Li, W. S. Yang and J. Caro, *Microporous and Mesoporous Materials*, 2014, 189, 210-215.
26. J. Cravillon, S. Münzer, S.-J. Lohmeier, A. Feldhoff, K. Huber and M. Wiebcke, *Chemistry of Materials*, 2009, 21, 1410-1412.
27. J. Cravillon, R. Nayuk, S. Springer, A. Feldhoff, K. Huber and M. Wiebcke, *Chemistry of Materials*, 2011, 23, 2130-2141.
28. R. W. Baker, *Membrane Technology and Applications*, John Wiley & Sons, Ltd, Menlo Park, California, 2nd edn., 2004.
29. N. A. H. M. Nordin, A. F. Ismail, A. Mustafa, P. S. Goh, D. Rana and T. Matsuura, *RSC Advances*, 2014, 4, 33292-33300.
30. A. F. Ismail and P. Y. Lai, *Separation and Purification Technology*, 2003, 33, 127-143.
31. A. F. Gross, E. Sherman and J. J. Vajo, *Dalton transactions*, 2012, 41, 5458.
32. Y. Pan, Y. Liu, G. Zeng, L. Zhao and Z. Lai, *Chemical communications*, 2011, 47, 2071-2073.
33. H. S. Khare and D. L. Burris, *Polymer*, 2010, 51, 719-729.
34. Y. Zhang, I. H. Musselman, J. P. Ferraris and K. J. Balkus, *Journal of Membrane Science*, 2008, 313, 170-181.
35. D. Ge and H. K. Lee, *Journal of chromatography. A*, 2011, 1218, 8490-8495.
36. G. C. Kapantaidakis, S. P. Kaldis, X. S. Dabou and G. P. Sakellariopoulos, *Journal of Membrane Science*, 1996, 110, 239-247.
37. A. F. Ismail and W. Lorna, *Separation and Purification Technology*, 2003, 30, 37-46.
38. B. Zornoza, S. Irusta, C. Téllez and J. n. Coronas, *Langmuir*, 2009, 25, 5903-5909.
39. Z. Bao, S. Alnemrat, L. Yu, I. Vasiliev, Q. Ren, X. Lu and S. Deng, *Journal of colloid and interface science*, 2011, 357, 504-509.
40. Z. R. Herm, J. A. Swisher, B. Smit, R. Krishna and J. R. Long, *Journal of the American Chemical Society*, 2011, 133, 5664-5667.
41. D. Fairen-Jimenez, S. A. Moggach, M. T. Wharmby, P. A. Wright, S. Parsons and T. Duren, *Journal of the American Chemical Society*, 2011, 133, 8900-8902.
42. T. Li, Y. Pan, K.-V. Peinemann and Z. Lai, *Journal of Membrane Science*, 2013, 425-426, 235-242.
43. N. A. H. M. Nordin, A. F. Ismail, A. Mustafa, R. S. Murali and T. Matsuura, *RSC Advances*, 2014, 4, 52530-52541.
44. S. A. Hashemifard, A. F. Ismail and T. Matsuura, *Chemical Engineering Journal*, 2011, 172, 581-590.
45. Q. Song, S. K. Nataraj, M. V. Roussanova, J. C. Tan, D. J. Hughes, W. Li, P. Bourgoïn, M. A. Alam, A. K. Cheetham, S. A. Al-Muhtaseb and E. Sivaniah, *Energy & Environmental Science*, 2012, 5, 8359-8369.